

# Attractor Solutions in $f(T)$ Cosmology

Mubasher Jamil,<sup>1,2,\*</sup> D. Momeni,<sup>2,†</sup> and Ratbay Myrzakulov<sup>2,‡</sup>

<sup>1</sup>*Center for Advanced Mathematics and Physics (CAMP),  
National University of Sciences and Technology (NUST), H-12, Islamabad, Pakistan*

<sup>2</sup>*Eurasian International Center for Theoretical Physics,  
Eurasian National University, Astana 010008, Kazakhstan*

**Abstract:** In this paper, we explore the cosmological implications of interacting dark energy model in a torsion based gravity namely  $f(T)$ . Assuming dark energy interacts with dark matter and radiation components, we examine the stability of this model by choosing different forms of interaction terms. We consider three different forms of dark energy: cosmological constant, quintessence and phantom energy. We then obtain several attractor solutions for each dark energy model interacting with other components. This model successfully explains the coincidence problem via the interacting dark energy scenario.

PACS numbers: 04.20.Fy; 04.50.+h; 98.80.-k

## I. INTRODUCTION

Its now well-accepted in astrophysics community that the observable universe is in a phase of rapid expansion whose rate of expansion is increasing, so called ‘accelerated expansion’. This conclusion has been drawn by numerous recent cosmological and astrophysical data findings of supernovae SNe Ia [1], cosmic microwave background radiations via WMAP [2], galaxy redshift surveys via SDSS [3] and galactic X-ray [4]. This phenomenon is commonly termed ‘dark energy’ (DE) in the literature, and suggests that a cosmic dark fluid possessing negative pressure and positive energy density. Although the phenomenon of dark energy in cosmic history is very recent  $z \sim 0.7$ , it has opened new areas in cosmology research. Two important problems like ‘fine tuning’ and ‘cosmic coincidence’ are related to dark energy. It is thought that the most elegant solution to DE paradigm is the Einstein’s cosmological constant [5] but it cannot resolve the two problems mentioned above. Hence cosmologists looked for other theoretical models by considering the dynamic nature of dark energy like quintessence scalar field [6], a phantom energy field [7] and f-essence [8]. Another interesting set of proposals to DE puzzle is the ‘modified gravity’ which was proposed after the failure of general relativity (GR). This new set of gravity theories passes several solar system and astrophysical tests successfully [9].

For the past few years, models based on DE interacting with dark matter or any other exotic component have gained great impetus. Such interacting DE models can successfully explain numerous cosmological puzzles including dynamic DE, phantom crossing, cosmic coincidence and cosmic age [10] and also in good compatibility with the astrophysical observations of cosmic microwave

background, supernova type Ia, baryonic acoustic oscillations and galaxy redshift surveys [11]. There are some criticisms on interacting DE models for not being favored from observations and that the usual  $\Lambda$ CDM model is favorable [12]. However the thermal properties of this model in various gravities have been discussed in literature [13]. The model in which dark energy interacts with two different fluids has been investigated in literature. In [14], the two fluids were dark matter and another was unspecified. However, in another investigation [15], the third component was taken as radiation to address the cosmic-triple-coincidence problem and study the generalized second law of thermodynamics. In a recent investigation, the authors investigated the coincidence problem in loop quantum gravity with triple interacting fluids including DE, dark matter and unparticle [16].

There is no need to construction a gravitational theory on a Riemannian manifold. A manifold can be divided to two separate but connected parts, one with Riemannian structure, with a definite metric and another part, with a non Riemannian structure and with torsion or non metricity. That part which has the zero Riemannian tensor but has non zero torsion is based on a tetrad basis, and defines a Weitzenbock spacetime.  $f(T)$  gravity is an alternative theory for GR, defined on the Weitzenbock non Riemannian manifold, working with torsion. This model firstly proposed by Einstein for unifying the electromagnetism and the gravity.. If  $f(T) = T$ , this theory so called teleparallel gravity [17, 18]. It has been shown that with linear  $T$ , this model have many similar features with GR and is in good agreement with some standard tests of the GR in solar system [17]. But introducing a general model  $f(T)$  backs to recent few years [19]. This model has many features, for example it has Birkhoff’s theorem [20]. As a thermodynamical view, there are many strange features. As it has been shown [21], in  $f(T)$  gravity, the famous formula of the entropy of the black holes is not valid. The reason backs to the non locally lorentz invariance of this theory [21, 22]. It shows that it is not possible to using from the Wald conjecture [23] as looking on entropy as a Noether charge in

\*Electronic address: mjamal@camp.nust.edu.pk

†Electronic address: d.momeni@yahoo.com; davidmathphys@yahoo.co.uk

‡Electronic address: rmyrzakulov@gmail.com; rmyrzakulov@csufresno.edu

$f(T)$ .

In this paper we study the triple coincidence problem: why we happen to live during this special epoch when  $\rho_\Lambda \sim \rho_m \sim \rho_r$ ? [24]. We investigate this problem in the framework of  $f(T)$  gravity.

Our plan in this paper as follows. In section II we introduce the basic equations as an autonomous dynamical system. In section III we choose a model for  $f(T)$  gravity. In section IV we working on numerical analysis of the stability and the evolution of the functions of the model in details. We conclude and summarize in section V.

## II. BASIC EQUATIONS

One suitable form of action for  $f(T)$  gravity in Weitzenbock spacetime is

$$S = \frac{1}{2\kappa^2} \int d^4x \sqrt{e}(T + f(T) + L_m)$$

Here  $e = \det(e_\mu^i)$ ,  $\kappa^2 = 8\pi G$  and  $e_\mu^i$  is the tetrad (vierbein) basis. The dynamical quantity of the model is the scalar torsion  $T$  and  $L_m$  is the matter Lagrangian. We start with the Friedmann equation in this form of the  $f(T)$  model [19]

$$H^2 = \frac{1}{1+2f_T} \left( \frac{\kappa^2}{3} \rho - \frac{f(T)}{6} \right), \quad (1)$$

where  $\kappa^2 = 8\pi G$ ,  $\rho = \rho_m + \rho_d + \rho_r$ , where  $\rho_m$ ,  $\rho_d$  and  $\rho_r$  represent the energy densities of matter, dark energy and the radiation.

Another FRW equation is

$$\dot{H} = -\frac{\kappa^2}{2} \left( \frac{\rho + p}{1 + f_T + 2Tf_{TT}} \right). \quad (2)$$

For a spatially flat universe ( $k = 0$ ), the total energy conservation equation is

$$\dot{\rho} + 3H(\rho + p) = 0, \quad (3)$$

where  $H$  is the Hubble parameter,  $\rho$  is the total energy density and  $p$  is the total pressure of the background fluid.

We assume a three component fluid containing matter, dark energy and radiation having an interaction. The corresponding continuity equations are [16]

$$\begin{aligned} \dot{\rho}_d + 3H(\rho_d + p_d) &= \Gamma_1, \\ \dot{\rho}_m + 3H\rho_m &= \Gamma_2, \\ \dot{\rho}_r + 3H(\rho_r + p_r) &= \Gamma_3, \end{aligned} \quad (4)$$

which satisfy collectively (3) such that  $\Gamma_1 + \Gamma_2 + \Gamma_3 = 0$ .

We define dimensionless density parameters via

$$x \equiv \frac{\kappa^2 \rho_d}{3H^2}, \quad y \equiv \frac{\kappa^2 \rho_m}{3H^2}, \quad z \equiv \frac{\kappa^2 \rho_r}{3H^2}. \quad (5)$$

The continuity equations (4) in dimensionless variables reduce to

$$\begin{aligned} \frac{dx}{dN} &= 3x \left( \frac{x + y + z + w_d x + w_r z}{1 + f_T + 2Tf_{TT}} \right) \\ &\quad - 3x(1 + w_d) + \frac{\kappa^2}{3H^3} \Gamma_1, \\ \frac{dy}{dN} &= 3y \left( \frac{x + y + z + w_d x + w_r z}{1 + f_T + 2Tf_{TT}} \right) \\ &\quad - 3y + \frac{\kappa^2}{3H^3} \Gamma_2, \\ \frac{dz}{dN} &= 3z \left( \frac{x + y + z + w_d x + w_r z}{1 + f_T + 2Tf_{TT}} \right) \\ &\quad - 3z(1 + w_r) + \frac{\kappa^2}{3H^3} \Gamma_3, \end{aligned} \quad (6)$$

where  $N \equiv \ln a$ , called the e-folding parameter. The coupling functions  $\Gamma_i$ ,  $i = 1, 2, 3$  are in general functions of the energy densities and the Hubble parameter i.e.  $\Gamma_i(H\rho_i)$ . The system of equations in (6) is analyzed by first equating them to zero to obtain the critical points. Next we perturb equations up to first order about the critical points and check their stability. Below for computation, we shall assume  $w_m = 0$ ,  $w_r = \frac{1}{3}$  and  $w_d$  to be a general non-zero but negative parameter. We are interested in stable critical points (i.e. those points for which all eigenvalues of Jacobian matrix are all negative) as these are attractor solutions of the dynamical system.

## III. $f(T)$ MODEL

To avoid analytic and computation problems, we choose a suitable  $f(T)$  expression which contains a constant, linear and a non-linear form of torsion, specifically

$$f(T) = 2C_1 \sqrt{-T} + \alpha T + C_2, \quad (7)$$

where  $\alpha$ ,  $C_1$  and  $C_2$  are arbitrary constants. The first and the third terms has the cosmological constant EoS in  $f(T)$  gravity. There are many kinds of such these models, reconstructed from different kinda of the dark energy models. For example this form of the  $f(T)$  may be inspired from a model for dark energy from proposed form of the Veneziano ghost[25]. But the linear term is needed to showing the differences between our results in  $f(T)$  gravity from the Einstein gravity. There are a large class of the models which some of them have exact solutions and are comparable with observational data. Here we choose these model for simplifying our numerical computations and further for easier discussion on the difference of our results with the same results in GR. It is the minimum model, but our equations have been written for a general  $f(T)$  action. It is possible by repeating the numerical steps as we done in this paper, discuss the stability of other models.

#### IV. ANALYSIS OF STABILITY IN PHASE SPACE

In this section, we will construct four models by choosing different coupling forms  $\Gamma_i$  and analyze the stability of the corresponding dynamical systems about the critical points. We shall plot the phase and evolutionary diagrams accordingly. For this reason, we must find the critical points of the (6), and then we linearize the system near the critical points up to first order.

##### A. Interacting model - I

We consider the model with the following interaction terms

$$\Gamma_1 = -6bH\rho_d, \quad \Gamma_2 = \Gamma_3 = 3bH\rho_d, \quad (8)$$

where  $b$  is a coupling parameter and we assume it to be a positive real number of order unity. Thus (8) says that both matter and radiation have increase in energy density with time while dark energy loses its energy density. Therefore it is a decay of dark energy into matter and radiation.

Using (8), the system (6) takes the form

$$\begin{aligned} \frac{dx}{dN} &= -3x(1+w_d) + 3x\left(\frac{x+y+z+w_dx+w_rz}{1+\alpha}\right) - 6bx, \\ \frac{dy}{dN} &= -3y + 3y\left(\frac{x+y+z+w_dx+w_rz}{1+\alpha}\right) + 3bx, \\ \frac{dz}{dN} &= -3z(1+w_r) + 3z\left(\frac{x+y+z+w_dx+w_rz}{1+\alpha}\right) + 3bx. \end{aligned} \quad (9)$$

The critical points for this model are obtained by equating the left hand sides of (9) to zero. We obtain four critical points:

- Point  $A_1$  :  $(\frac{(1+\alpha)(1+w_d+2b)}{1+w_d}, 0, 0)$ ,
- Point  $B_1$  :  $(0, 0, 0)$ ,
- Point  $C_1$  :  $(0, (1-b)(1+\alpha), 0)$ ,
- Point  $D_1$  :  $(0, 0, \frac{3}{4}(1+\alpha)(\frac{4}{3}-b))$

The eigenvalues of the Jacobian matrix for these critical points are:

- Point  $A_1$  :  $\lambda_1 = 3(1+w_d+2b), \lambda_2 = 3(w_d+3b), \lambda_3 = -1 + 3(w_d+3b)$ ,
- Point  $B_1$  :  $\lambda_1 = 3(b-1), \lambda_2 = -3(b-1), \lambda_3 = -3(1+2b+w_d)$ ,
- Point  $C_1$  :  $\lambda_1 = -1, \lambda_2 = 3(1-b), \lambda_3 = -3(w_d+3b)$ ,
- Point  $D_1$  :  $\lambda_1 = 1, \lambda_2 = 4-3b, \lambda_3 = 1-3w_d-9b$

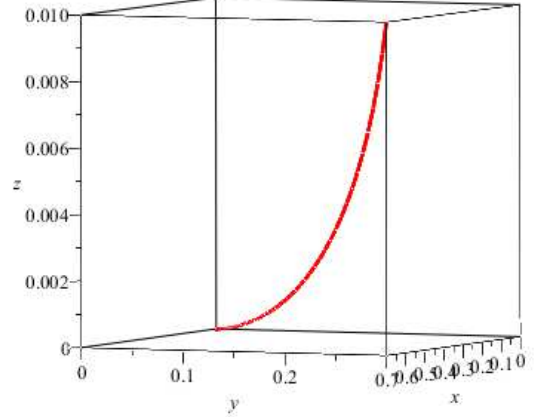


FIG. 1: Model I: Phase space for  $w_d = -1.2, b = 0.5, \alpha = 0.5$ . It shows an attractor behavior.

Point  $A_1$  is stable when one of these conditions is satisfied:

$$w_d < -3, \quad b < 1/18. \quad (10)$$

$$w_d \geq -3, \quad w_d < -10/9, \quad b < 1/18. \quad (11)$$

$$w_d \geq -\frac{10}{9}, \quad w_d < 0, \quad b < -\frac{1}{2}(1+w_d). \quad (12)$$

$B_1$  is an unstable critical point since if  $b > 1$  then  $\lambda_1 > 0$  but  $\lambda_2 < 0$ .  $C_1$  is stable if  $b > 1, w_d > -3b$ . Similarly  $D_1$  is unstable since  $\lambda_1 > 0$ .

In figures (1-6), we plot the parameters of model-I. In figure 1, we observe that the dimensionless density parameters evolve from their currently observed values to vanishing densities. In figure-2, we observe similar behavior when plotted against e-folding parameter: the density parameters evolve from their current values to zero. In figure-1, we deal with phantom energy, in figure-3, the quintessence case while in figure-5, the cosmological constant case.

##### B. Interacting model - II

We study another model with the choice of the interaction terms

$$\Gamma_1 = -3bH\rho_d, \quad \Gamma_2 = 3bH(\rho_d - \rho_m), \quad \Gamma_3 = 3bH\rho_m. \quad (13)$$

This model effectively describes the situation when dark energy loses energy density to matter while the radiation

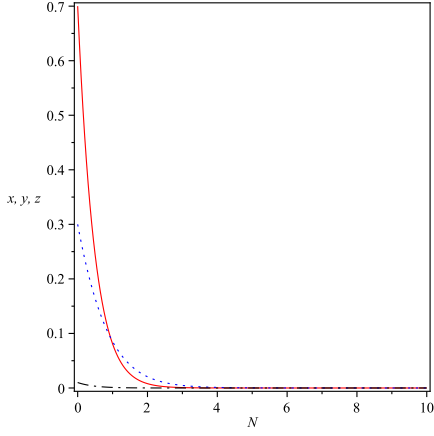


FIG. 2: Model I: variation of  $x, y, z$  as a function of the  $N = \ln(a)$ . The initial conditions chosen are  $x(0) = 0.7, y(0) = 0.3, z(0) = 0.01, w_d = -1.2$  and  $b = 0.5$ .

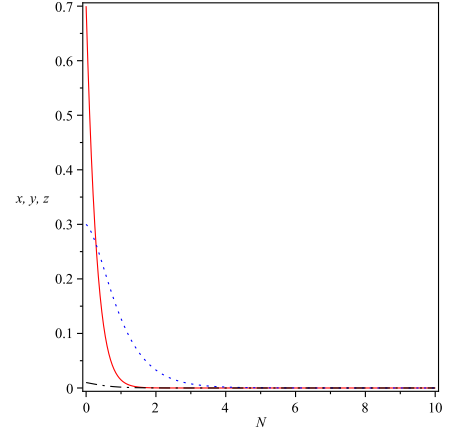


FIG. 4: Model I: variation of  $x, y, z$  as a function of the  $N = \ln(a)$ . The initial conditions chosen are  $x(0) = 0.7, y(0) = 0.3, z(0) = 0.01, w_d = -0.5$  and  $b = 0.5$ .

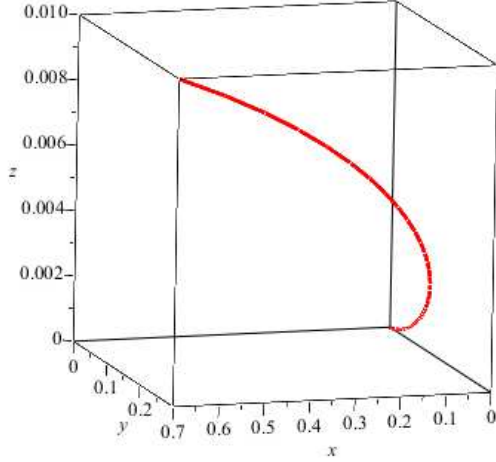


FIG. 3: Model I: Phase space for  $w_d = -0.5, b = 0.5, \alpha = 0.5$ .

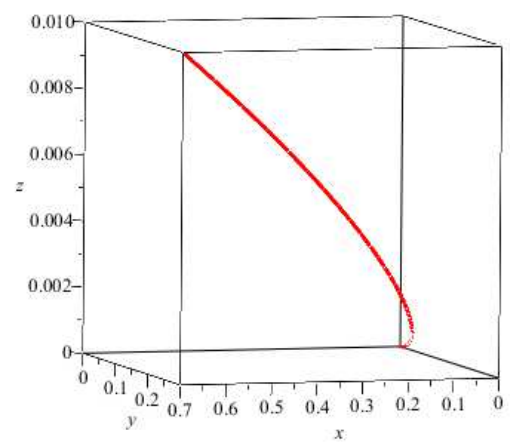


FIG. 5: Model I: Phase space for  $w_d = -1, b = 0.5, \alpha = 0.5$ .

density increases due to interaction with the matter.

$$\frac{dx}{dN} = 3x \left( \frac{x+y+z+w_dx+w_rz}{1+\alpha} - 3bx - 3x(1+w_d) \right) \quad (14)$$

$$\frac{dy}{dN} = 3y \left( \frac{x+y+z+w_dx+w_rz}{1+\alpha} + 3b(x-y) - 3y \right) \quad (15)$$

$$\frac{dz}{dN} = 3z \left( \frac{x+y+z+w_dx+w_rz}{1+\alpha} + 3by - 3z(1+w_r) \right) \quad (16)$$

There are four critical points:

- Point  $A_2$  :  $(0, 0, 0)$ ,

- Point  $B_2$  :  $(0, 0, 1 + \alpha)$ ,
- Point  $C_2$  :  $(0, (1 - 3b)(1 + \alpha), 3b(1 + \alpha))$ ,
- Point  $D_2$  :  $\left( -\frac{3(2+w_d)(b-w_d-1)(b-w_d-7/3)(\alpha+1)}{3w_d^3+(16-3b)w_d^2+(-6b+27)w_d+14+b^2+b}, \right.$   
 $\left. -\frac{b3(\alpha+1)(b-w_d-7/3)(b-w_d-1)}{3w_d^3+(16-3b)w_d^2+(-6b+27)w_d+14+b^2+b}, \frac{3(\alpha+1)(b-w_d-1)b^2}{14+16w_d^2-6w_db+b^2-3w_d^2b+3w_d^3+27w_d+b} \right)$

The eigenvalues of the Jacobian matrix for these critical points are:

- Point  $A_2$  :  $\lambda_1 = -4, \lambda_2 = -3(1+b), \lambda_3 = 3(1+w_d-b)$ ,
- Point  $B_2$  :  $\lambda_1 = 4, \lambda_2 = 1-3b, \lambda_3 = 7+3(w_d-b)$ ,
- Point  $C_2$  :  $\lambda_1 = 3(1+b), \lambda_2 = 3b-1, \lambda_3 = 3(w_d+2)$ ,

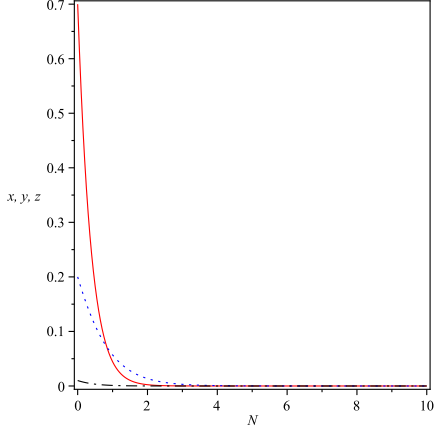


FIG. 6: Model I: variation of  $x, y, z$  as a function of the  $N = \ln(a)$ . The initial conditions chosen are  $x(0) = 0.7, y(0) = 0.3, z(0) = 0.01, w_d = -1$  and  $b = 0.5$ .

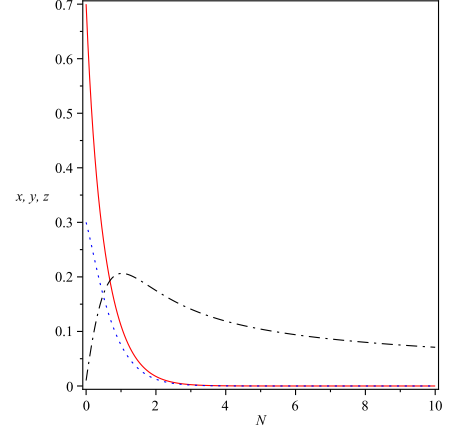


FIG. 8: Model II: variation of  $x, y, z$  as a function of the  $N = \ln(a)$ . The initial conditions chosen are  $x(0) = 0.7, y(0) = 0.3, z(0) = 0.01, w_d = -1.2$  and  $b = 0.5$ .

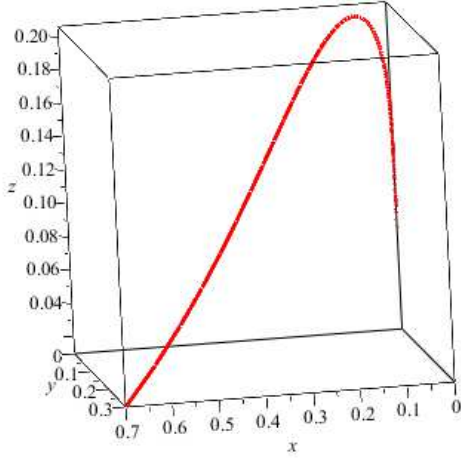


FIG. 7: Model II: Phase space for  $w_d = -1.2, b = 0.5, \alpha = 0.5$ .

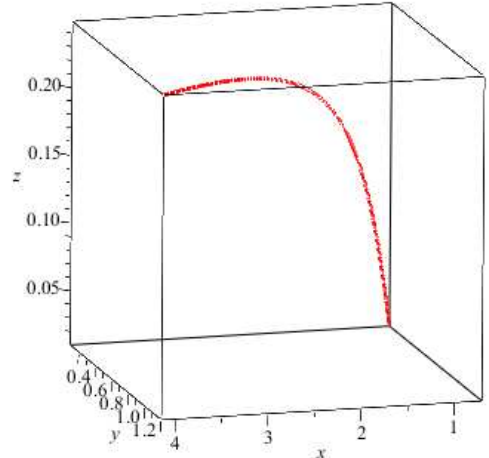


FIG. 9: Model II: Phase space for  $w_d = -0.5, b = 0.5, \alpha = 0.5$ .

- Point  $D_2$  :  $\lambda_1 = -3(w_d+2), \lambda_2 = 3(b-w_d-1), \lambda_3 = -7-3(b-w_d)$

$A_2, D_2$  are conditionally stable if  $b > 1+w_d$  (for  $A_2$ ) and  $w_d > -2$  and  $b < 1+w_d$  (for  $D_2$ ). But  $B_2$  and  $C_2$  are unstable since  $\lambda_1 > 0$ .

In figures (7-12), we show the dynamics of Model-II. Attractor solutions are shown in figures 7,9 and 11. In figure 8, we see that the energy density of dark energy decays like quintessence. Also the energy density of radiation first increases till  $N \sim 1.6$  and then starts decreasing. The matter density always decreases and approaches zero nearly  $N \sim 3$ . In figure 10, the energy density of dark energy increases rapidly behaving like phantom energy, energy density of matter rises almost

exponentially at later times, while radiation density increases slower compared to both matter and dark energy. These novel behaviors appear on account of interaction between three components. In figure 12, the dark energy density behaves like quintessence, while matter and radiation density falls with expansion.

### C. Interacting Model - III

Let us take the interaction terms [16]

$$\Gamma_1 = -6b\kappa^2 H^{-1} \rho_d \rho_r, \quad \Gamma_2 = \Gamma_3 = 3b\kappa^2 H^{-1} \rho_d \rho_r. \quad (17)$$

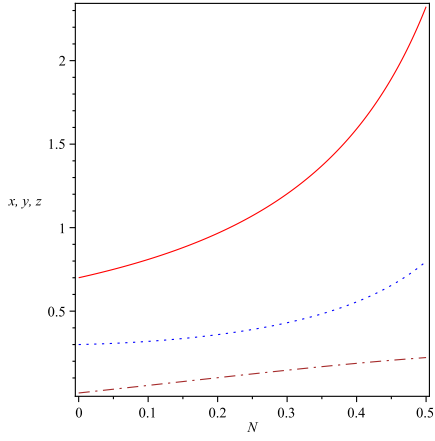


FIG. 10: Model II: variation of  $x, y, z$  as a function of the  $N = \ln(a)$ . The initial conditions chosen are  $x(0) = 0.7, y(0) = 0.3, z(0) = 0.01, w_d = -0.5$  and  $b = 0.5$ .

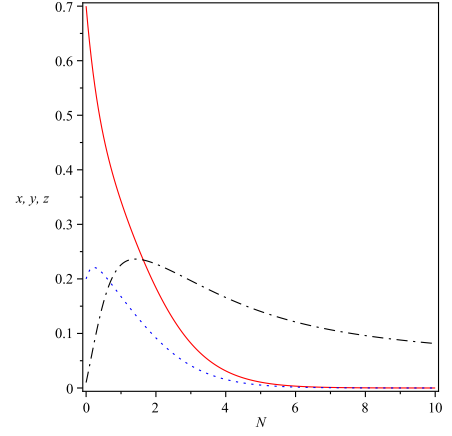


FIG. 12: Model II: variation of  $x, y, z$  as a function of the  $N = \ln(a)$ . The initial conditions chosen are  $x(0) = 0.7, y(0) = 0.3, z(0) = 0.01, w_d = -1$  and  $b = 0.5$ .

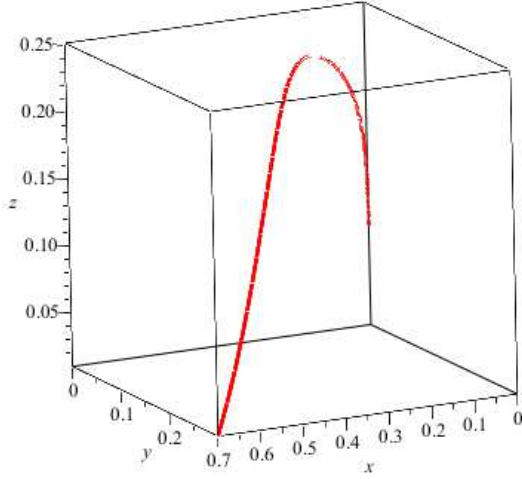


FIG. 11: Model II: Phase space for  $w_d = -1, b = 0.5, \alpha = 0.5$ .

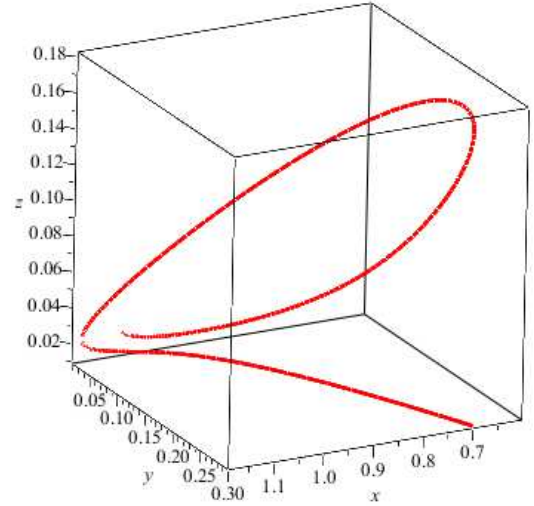


FIG. 13: Model III: Phase space for  $w_d = -1.2, b = 0.5, \alpha = 0.5$ .

The system in (6) takes the form

$$\begin{aligned} \frac{dx}{dN} &= 3x \left( \frac{x+y+z+w_dx+w_rz}{1+\alpha} \right) - 3x - 3w_dx - 18bxz, \\ \frac{dy}{dN} &= 3y \left( \frac{x+y+z+w_dx+w_rz}{1+\alpha} \right) - 3y + 9bxz, \\ \frac{dz}{dN} &= 3z \left( \frac{x+y+z+w_dx+w_rz}{1+\alpha} \right) - 3z - 3w_rz + 9bxz. \end{aligned} \quad (18)$$

There are six critical points:

- Point  $A_3 : (0, 0, 0)$ ,
- Point  $B_3 : (0, 1 + \alpha, 0)$ ,
- Point  $C_3 : (0, 0, 1 + \alpha)$ ,

- Point  $D_3 : (1 + \alpha, 0, 0)$ ,
- Point  $E_3 : \left( \frac{4}{9b}, -\frac{2(1+w_d)}{9b}, -\frac{1+w_d}{6b} \right)$ ,
- Point  $F_3 : \left( \frac{(w_d+6b\alpha+6b-\frac{1}{3})}{b(6b\alpha+6b-\frac{1}{3}+2w_d)}, \frac{-3b\alpha-3b+36b^2\alpha^2+18b^2\alpha^2+9w_db\alpha+18b^2+w_d^2-2w_d\frac{1}{3}+9w_db+\frac{1}{9}}{3b(6b\alpha+6b-\frac{1}{3}+2w_d)}, -\frac{w_d(3b\alpha+3b-\frac{1}{3}+w_d)}{3b(6b\alpha+6b-\frac{1}{3}+2w_d)} \right)$

The eigenvalues of the Jacobian matrix for these critical points are:

- Point  $A_3 : \lambda_1 = -3, \lambda_2 = -4, \lambda_3 = -3(1 + w_d)$ ,
- Point  $B_3 : \lambda_1 = 3, \lambda_2 = -1, \lambda_3 = -3w_d$ ,

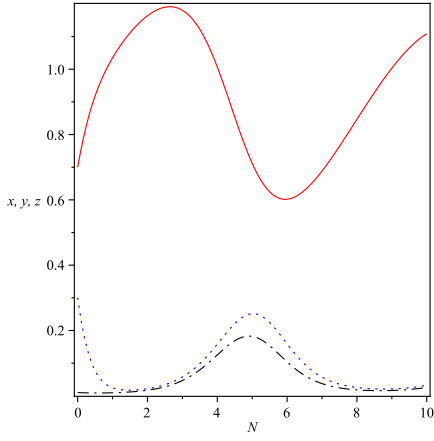


FIG. 14: Model III: variation of  $x, y, z$  as a function of the  $N = \ln(a)$ . The initial conditions chosen are  $x(0) = 0.7, y(0) = 0.3, z(0) = 0.01, w_d = -1.2$  and  $b = 0.5$ .

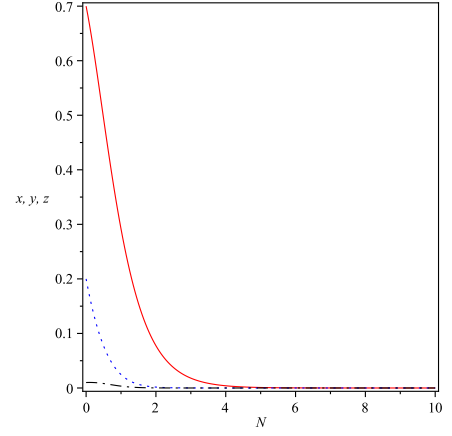


FIG. 16: Model III: variation of  $x, y, z$  as a function of the  $N = \ln(a)$ . The initial conditions chosen are  $x(0) = 0.7, y(0) = 0.3, z(0) = 0.01, w_d = -0.5$  and  $b = 0.5$ .

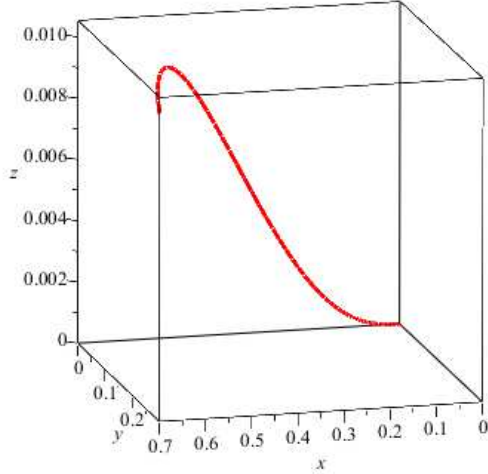


FIG. 15: Model III: Phase space for  $w_d = -0.5, b = 0.5, \alpha = 0.5$ .

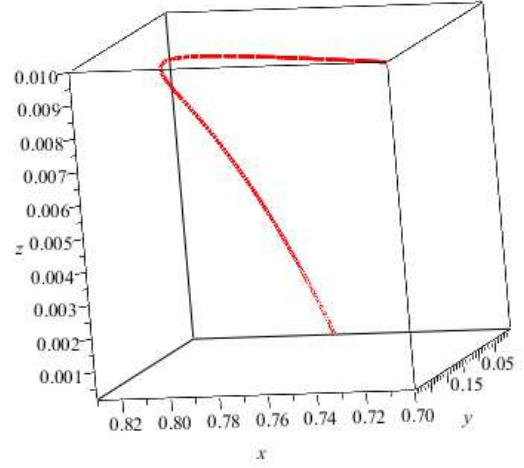


FIG. 17: Model III: Phase space for  $w_d = -1, b = 0.5, \alpha = 0.5$ .

- Point  $C_3$  :  $\lambda_1 = 3w_d, \lambda_2 = 3(1 + w_d), \lambda_3 = 9b\alpha + 9b - 1 + 3w_d$ ,
- Point  $D_3$  :  $\lambda_1 = 4, \lambda_2 = 1 - 9b - 9b\alpha, \lambda_3 = -9b\alpha - 9b + 1 - 3w_d$ .

$A_3$  is stable for  $w_d > -1$ .  $B_3, D_3$  are unstable.  $C_3$  is conditionally stable when  $w_d < -1, b < \frac{1-3w_d}{9(1+\alpha)}$ .

In figures (13-18), we have plotted the cosmological parameters of model-III. In figures 13, 15 and 17, we show the attractor solutions of the differential equations. In figure 14, we observe the oscillatory behavior of dark energy and other cosmic components. It shows that when DE energy density decays then corresponding densities of dark matter and radiation increases and

vice versa. Figure 16 shows that all forms of energy densities vanish by  $N \sim 4.5$ . From figure 18, the radiation density stays zero while matter energy density decreases and vanishes by  $N \sim 2$ . The dark energy density increases by  $N \sim 2$  while it decreases and stays constant at later epochs.

#### D. Interacting Model - IV

Consider another model with the interaction terms [16]

$$\begin{aligned}\Gamma_1 &= -3b\kappa^2 H^{-1} \rho_d \rho_r, \\ \Gamma_2 &= 3b\kappa^2 H^{-1} (\rho_d \rho_r - \rho_m \rho_r), \\ \Gamma_3 &= 3b\kappa^2 H^{-1} \rho_m \rho_r.\end{aligned}\tag{19}$$

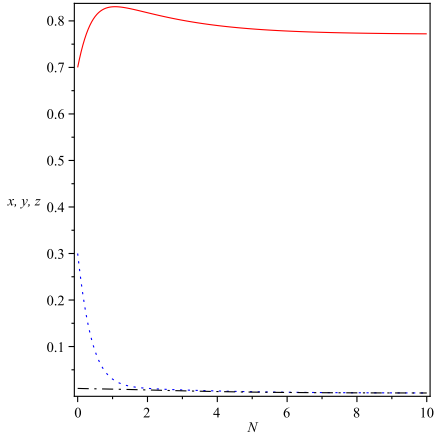


FIG. 18: Model III: variation of  $x, y, z$  as a function of the  $N = \ln(a)$ . The initial conditions chosen are  $x(0) = 0.7, y(0) = 0.3, z(0) = 0.01, w_d = -1$  and  $b = 0.5$ .

The system in (6) takes the form

$$\begin{aligned}\frac{dx}{dN} &= 3x \left( \frac{x+y+z+w_dx+w_rz}{1+\alpha} \right) - 3x - 3w_dx - 9bxz, \\ \frac{dy}{dN} &= 3y \left( \frac{x+y+z+w_dx+w_rz}{1+\alpha} \right) - 3y + 9b(xz - y^2), \\ \frac{dz}{dN} &= 3z \left( \frac{x+y+z+w_dx+w_rz}{1+\alpha} \right) - 3z - 3w_rz + 9byz.\end{aligned}$$

There are seven critical points:

- Point  $A_4 : (0, 0, 0)$ ,
- Point  $B_4 : (1 + \alpha, 0, 0)$ ,
- Point  $C_4 : (0, 1 + \alpha, 0)$ ,
- Point  $D_4 : (0, 0, 1 + \alpha)$ ,
- Point  $E_4 : \left( \frac{1}{3} \frac{w_d}{b(1+w_d)}, \frac{4}{9b}, -\frac{1}{3} \frac{1+w_d}{b} \right)$ ,
- Point  $F_4 : \left( \frac{w_d+3b+3b\alpha-1/3}{3b}, -\frac{(-\frac{1}{3}+w_d)(w_d+3b+3b\alpha-\frac{1}{3})}{3b(3b+3b\alpha-\frac{1}{3})}, \frac{w_d(-\frac{1}{3}+w_d)}{3b(3b+3b\alpha-\frac{1}{3})} \right)$ ,
- Point  $G_4 : (0, \frac{4}{9b}, -\frac{1}{3b})$ .

For points  $A_4, B_4, C_4, D_4, G_4$ , the eigenvalues of the Jacobian matrix are

- Point  $A_4 : \lambda_1 = -3, \lambda_2 = -4, \lambda_3 = -3(1 + w_d)$ ,
- Point  $B_4 : \lambda_1 = 3w_d, \lambda_2 = 3(1 + w_d), \lambda_3 = 3w_d - 1$ ,
- Point  $C_4 : \lambda_1 = 3, \lambda_2 = -3w_d, \lambda_3 = 9b(1 + \alpha) - 1$ ,
- Point  $D_4 : \lambda_1 = 3(1 + w_d), \lambda_2 = -9b - 9b\alpha + 1, \lambda_3 = -3w_d - 9b - 9b\alpha + 1$ ,

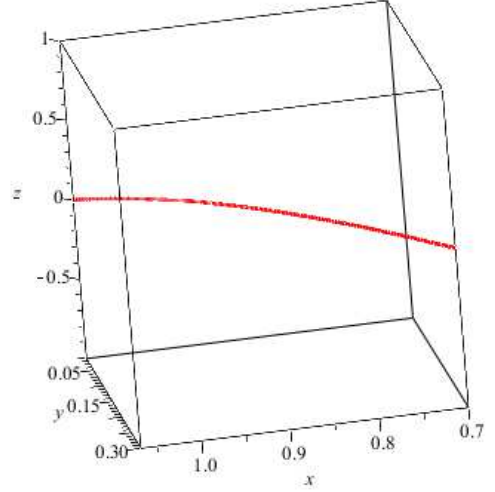


FIG. 19: Model IV: Phase space for  $w_d = -1.2, b = 0.5, \alpha = 0.5$ .

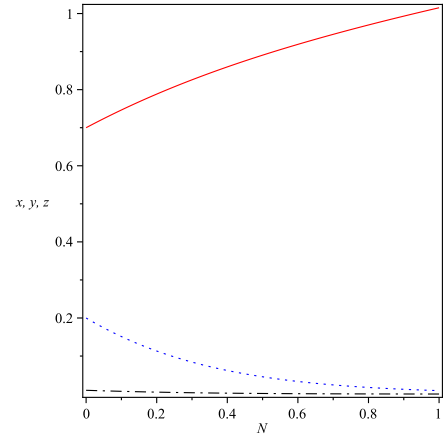


FIG. 20: Model IV: variation of  $x, y, z$  as a function of the  $N = \ln(a)$ . The initial conditions chosen are  $x(0) = 0.7, y(0) = 0.3, z(0) = 0.01, w_d = -1.2$  and  $b = 0.5$ .

- Point  $G_4 : \lambda_1 = -3w_d,$   
 $\lambda_2 = \frac{\sqrt{3}\sqrt{b(1+\alpha)(3b\alpha+3b/3\alpha-4/9+3b+b)}}{b(1+\alpha)},$   
 $\lambda_3 = -\frac{\sqrt{3}\sqrt{b(1+\alpha)(3b\alpha+3b/3\alpha-4/9+3b+b)}}{b(1+\alpha)}$

It is observed that in this model,  $A_4$  is stable for  $w_d > -1$ ,  $B_4$  is stable for  $w_d < -1$ .  $C_4$  is unstable.  $D_4$  is stable for  $w_d < -1, b > \frac{1}{9(1+\alpha)}$ . It's not possible to determine the stability of the point  $E_4$ . But  $G_4$  is unstable.

In figures (19-24), we give description about model-IV. Figures 19,21,23 represent the phase space diagrams for different forms of dark energy. Figures 22 and 24 shows that energy density of dark energy decreases while in figure 20, the density of DE increases. It's the typical



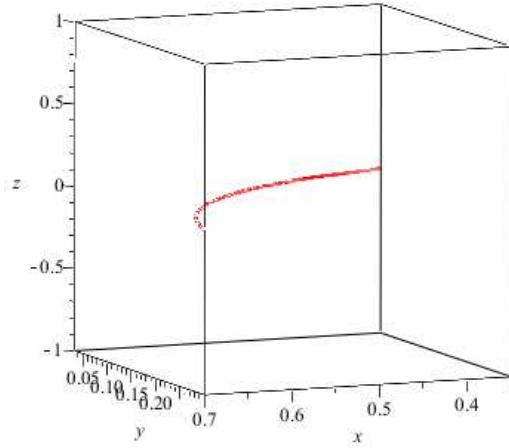


FIG. 21: Model IV: Phase space for  $w_d = -0.5, b = 0.5, \alpha = 0.5$ .

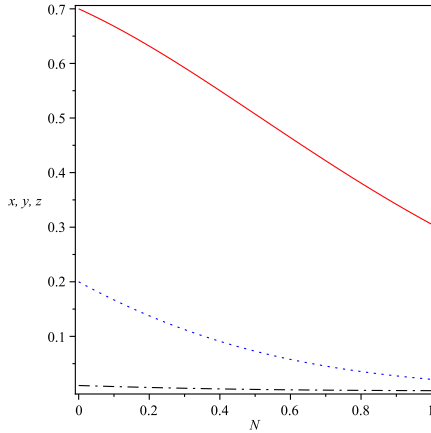


FIG. 22: Model IV: variation of  $x, y, z$  as a function of the  $N = \ln(a)$ . The initial conditions chosen are  $x(0) = 0.7, y(0) = 0.3, z(0) = 0.01, w_d = -0.5$  and  $b = 0.5$ .

behavior of the phantom fields. Thus, our model predicts the correct evolutionary scheme for the DE density in regime of phantom.

## V. DISCUSSION

$f(T)$  gravity is a powerful and novel theory for explanation of the acceleration expansion of the universe. IN this paper we discuss the stability of the interactive models of the dark energy, matter and radiation in a

FRW model, for a general  $f(T)$  theory. We derived the equations and show that why we have some attractor solutions for some specific forms of the interactions. We

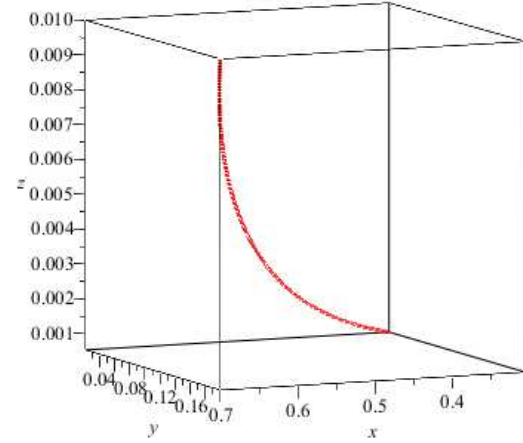


FIG. 23: Model IV: Phase space for  $w_d = -1, b = 0.5, \alpha = 0.5$ .

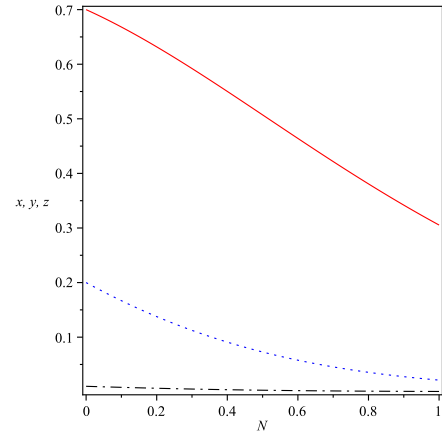


FIG. 24: Model IV: variation of  $x, y, z$  as a function of the  $N = \ln(a)$ . The initial conditions chosen are  $x(0) = 0.7, y(0) = 0.3, z(0) = 0.01, w_d = -1$  and  $b = 0.5$ .

numerically integrate the equations and show that the evolution of the dark energy density mimics three diffract behaviors phantom, quintessence and cosmological constant in some interactive forms. Since the phase space of the system of the evolutionary equations has a definitive end point, trackers are exist and depending on the initial conditions, there are different kinds of the trackers.

- [3] M. Tegmark et al., Phys. Rev. D 69, 103501 (2004).
- [4] S. W. Allen et al., Mon. Not. Roy. Astron. Soc. 353, 457 (2004).
- [5] V. Sahni, A. Starobinsky, Int. J. Mod. Phys. D 9, 373 (2000); P. J. Peebles, B. Ratra, Rev. Mod. Phys. 75, 559 (2003).
- [6] B. Ratra, P. J. E. Peebles, Phys. Rev. D 37, 3406 (1988); C. Wetterich, Nucl. Phys. B 302, 668 (1988); A. R. Liddle, R. J. Scherrer, Phys. Rev. D 59, 023509 (1999).
- [7] R. R. Caldwell, Phys. Lett. B 545, 23 (2002); R. R. Caldwell, M. Kamionkowski, N. N. Weinberg, Phys. Rev. Lett. 91, 071301 (2003).
- [8] M. Jamil, Y. Myrzakulov, O. Razina, R. Myrzakulov, Astrophys. Space Sci. 336, 315 (2011); M. Jamil, D. Momeni, N. S. Serikbayev, R. Myrzakulov, Astrophysics and Space Science DOI: 10.1007/s10509-011-0964-7 [arXiv:1112.4472v1 [physics.gen-ph]].
- [9] S. Nojiri, S. D. Odintsov, Phys. Rept. 505, 59 (2011); S. Capozziello, M. De Laurentis, arXiv:1108.6266v2 [gr-qc]; T. Clifton, P. G. Ferreira, A. Padilla, C. Skordis, arXiv:1106.2476v2 [astro-ph.CO]
- [10] M. Jamil, M.A. Rashid, Eur. Phys. J. C 60, 141 (2009); M. Jamil, M.A. Rashid, Eur. Phys. J. C 58, 111 (2008); M. Jamil, M.A. Rashid, Eur. Phys. J. C 56, 429 (2008); M. Jamil, F. Rahaman, Eur. Phys. J. C 64, 97 (2009); M. Jamil, Int. J. Theor. Phys. 49, 144 (2010); M. Jamil, M. Raza, U. Debnath, Astrophys. Space Sci. 337, 799 (2012).
- [11] H. Wei, S. N. Zhang, Phys. Lett. B 654, 139 (2007); M-L Tong, Y Zhang, Z-W Fu, Class. Quant. Grav. 28, 055006 (2011); Y-H Li, J-Z Ma, J-L. Cui, Z. Wang, X. Zhang, Sci. China Phys. Mech. Astron. 54, 1367 (2011); H. Wei, Phys. Lett. B 691, 173 (2010); S. M. R. Micheletti, JCAP 1005, 009 (2010); C. Feng, B. Wang, E. Abdalla, R-K. Su, Phys. Lett. B 665, 111 (2008); L. Amendola, C. Quercellini, D. T-Valentini, A. Pasqui, Astrophys.J. 583, L53 (2003)
- [12] G. Olivares, F. A-Barandela, D. Pavon, Phys. Rev. D 77, 063513 (2008).
- [13] M. Jamil, A. Sheykhi, M. U Farooq, Int. J. Mod. Phys. D 19, 1831 (2010); K. Karami, A. Sheykhi, M. Jamil, Z. Azarmi, M. M. Soltanzadeh, Gen. Relativ. Grav. 43, 27 (2011); M. Jamil, E. N. Saridakis, JCAP 1007, 028 (2010)
- [14] N. Cruz, S. Lepe, F. Pena, Phys. Lett. B 699, 135 (2011); N. Cruz, S. Lepe, F. Pena, Phys. Lett. B 663, 338 (2008).
- [15] M. Jamil, E. N. Saridakis, M.R. Setare, Phys. Rev. D 81, 023007 (2010)
- [16] M. Jamil, D. Momeni, M. A. Rashid, Eur. Phys. J. C 71, 1711 (2011).
- [17] K. Hayashi, T. Shirafuji, Phys. Rev. D 19, 35243553 (1979) ; K. Hayashi, T. Shirafuji, Phys. Rev. D 24, 33123314 (1981)
- [18] F. Hehl, P. von der Heyde and G. Kerlick, Rev. Mod. Phys. 48, 393416 (1976) .
- [19] R.Ferraro, F.Fiorini,Phys.Rev.D 75,084031(2007); R.Ferraro, F.Fiorini,Phys.Rev.D 78,124019(2008).
- [20] X.Meng, Y.Wang, Eur.Phys.J. C71 (2011) 1755.
- [21] R.Miao, M.Li, Y.Miao, JCAP11(2011)033 .
- [22] B.Li,T.P.Sotiriou,J.D.Barrow,Phys.Rev.D 83,064035(2011).
- [23] R.M.Wald,Phys.RevD 48,R3427(1993)
- [24] N. Arkani-Hamed, L. J. Hall, C. Kolda, H. Murayama, Phys. Rev. Lett. 85, 4434 (2000)
- [25] K. Karami, A. Abdolmaleki, arXiv:1202.2278.